Acta Ophthalmologica

Acta Ophthalmologica 2021

Profiling neovascular age-related macular degeneration choroidal neovascularization lesion response to anti-vascular endothelial growth factor therapy using SSOCTA

Reinhard Told, Gregor S. Reiter, Tamara J. Mittermüller, Markus Schranz, Adrian Reumueller, Ferdinand G. Schlanitz, Günther Weigert, Andreas Pollreisz, Stefan Sacu and Ursula Schmidt-Erfurth

Department of Ophthalmology and Optometry, Vienna Clinical Trial Center (VTC), Medical University of Vienna, Vienna, Austria

ABSTRACT.

Purpose: **To identify the changes in distinct vascular parameters of choroidal neovascularization (CNV) in eyes with treatment-naïve neovascular age-related macular degeneration (nAMD) during the primary response to anti-VEGF therapy using aflibercept.**

Methods: **Patients were prospectively followed during the first 3 months according to a standardized protocol with mandatory visits at days 7 and 14 after each anti-VEGF treatment up to day 90. Fourteen eyes were seen in addition at days 1 and 3 post-initial injection. Aflibercept was administered at baseline (BL), day 30 and 60. 6 × 6mm SSOCTA (PlexElite, Zeiss) images were acquired. Using the semi-automated AngioTool, CNV area, vessel area, vessel density (VD), the number of junctions, junctions density, total vessel length, average vessel length, total number of endpoints and lacunarity were assessed.**

Results: **Thirty-two consecutive patients presenting with treatment-naïve, SSOCTA-positive CNV lesions were included. Close follow-up showed a characteristic neovascular response curve with a dynamic decrease in lesion size within days and a reactive increase following 2 weeks after initial treatment. An undulating pattern was seen for all neovascular parameters except for vascular density, with variable statistical significance. Due to a flattening of the therapeutic response as early as after the second treatment, CNV lesion size and most of the related parameters had an increase in activity above baseline values at the end of the loading phase. Lesion size was the leading feature of reactivation by a mean increase of 19.3% after three monthly aflibercept injections. Subgroup analysis based on lesion size revealed a significant correlation between best-corrected visual acuity and quantitative change in lesion size over time, but not baseline size.**

Conclusions: **Using SSOCTA, a morphologic neovascular response pattern can be identified in anti-VEGF treatment of CNV. A synchronized early decrease and consecutive reactivation in a large spectrum of neovascular biomarkers including size and internal structure are visualized in a qualitative and quantitative manner. SSOCTA analyses allow new insights in CNV morphology changes and therapeutic response.**

Key words: biomarker – choroidal neovascularization – loading phase – neovascular age-related macular degeneration – SSOCTA

Acta Ophthalmol. 2021: 99: e240–e246

doi: 10.1111/aos.14554

Introduction

Intravitreal anti-vascular endothelial growth factor (VEGF) therapy is the gold standard for treating neovascular age-related macular degeneration (nAMD) treatment. With a large variability in numbers of intravitreal injections performed in patients with nAMD in clinical routine, biomarkers for monitoring adequate response to treatment and to indicate the need for retreatment are crucial for an efficient therapy of the AMD population as well as each individual patient. Optical coherence tomography (OCT) has already revolutionized nAMD diagnostics and treatment, and features such as central retinal thickness, pigment epithelial detachment, subretinal and intraretinal fluid are used as surrogate parameters to determine treatment response with OCT offering a vascular endothelial growth factor '(VEGF)-meter' (Rosenfeld 2016). A tight correlation of OCT-based features with treatment outcomes has recently been confirmed by artificial intelligence (Schmidt-Erfurth et al. 2018). With the introduction of OCT angiography (OCTA; Zotter et al. 2011; Jia et al. 2012), an essential tool has become available to directly visualize the choroidal neovascularization (CNV) complex non-invasively. Preliminary data suggest that the latest advances in OCTA based on swept-source technology (SSOCTA) have higher sensitivity and specificity in detecting CNV compared with spectral domain (SD)

OCTA (Told et al. 2016). The sensitivity levels for CNV detection published in the literature range between 32% and 53% using SDOCTA (Told et al. 2016; Babiuch et al. 2019). With the latest advancements in OCTA technology (SSOCTA), sensitivity increases to 68–86% (Moult et al. 2014; Gong et al. 2016; Told et al. 2016). Worth mentioning is the fact that using manual segmentation in SDOCTA volumes increased sensitivity further, to 92% (Babiuch et al. 2019), an investigation still pending in SSOCTA. SSOCTA further allows advanced and more detailed identification of characteristic CNV-related features compared with SDOCTA (Novais et al. 2016; Miller et al. 2017; Cicinelli et al. 2019). When it comes to comparing the current gold standard (Chakravarthy & Williams 2013; Schmidt-Erfurth et al. 2014) for CNV detection, which is fluorescein angiography (FA) and if needed indocyanine green angiography (ICGA), with non-invasive angiography, data are limited but indicate that both, FA and ICGA, are still superior to OCTA regarding exudative CNV detection (de Carlo et al. 2015; Told et al. 2018). However, as shown recently, there was no statistically significant difference in measurements from FA/ICGA and SSOCTA images after a deep learning-based image registration had been performed (Told et al. 2019). This progress in technology has raised hopes firstly that the current dye-based gold standard fluorescein and indocyanine green angiography can potentially be replaced by OCTA and secondly that new biomarkers for a detailed assessment of CNV morphology may become available. OCT imaging merely visualizes the secondary fluid-related consequences of CNV activity as well as the resolution of fluid under therapy, but does not offer any insight into the vascular biology and response of CNV to a treatment, which has originally been labelled as "anti-angiogenic". Fluid, however, does not correlate in a 1:1 fashion with visual acuity, nor does it explain the impact of VEGF inhibition on the neovascular biology (Schmidt-Erfurth & Waldstein 2016). OCTA with its intrinsic potential to visualize a wide spectrum of vascular patterns in great detail offers a unique opportunity to increase our insight into therapeutic efficacy. This study aimed at profiling the morphologic CNV lesion response during its most sensitive phase, that is the aflibercept loading phase in treatment-naïve CNV in a prospective and standardized manner using the most advanced OCTA technology. Moreover, CNV characteristics and best-corrected visual acuity (BCVA) are correlated to identify the adequate OCTA-based parameters to guide treatment in the near future.

Methods

Thirty-two consecutive patients with treatment-naïve nAMD presenting at the Ophthalmology Department of the Medical University of Vienna, Vienna, Austria were included in this prospective case series after signing an informed consent. The study protocol was approved by the Ethics Committee of the Medical University of Vienna, Vienna, Austria, and the study was conducted in adherence to the Declaration of Helsinki including current revisions and the Good Clinical Practice (GCP) guidelines.

Inclusion criteria

Inclusion criteria were age $\geq$50 years and diagnosis of actively leaking, treatment-naïve type 1 or type 2 nAMD or mixed type CNV due to AMD, clear ocular media, and the willingness to give informed consent to participate in this study. Any pretreatment or other ocular disease was considered an exclusion criterion. Patients with a refractive error greater than $\pm$6 dioptres (spherical equivalent), or an allergy to intravenous dye (fluorescein or indocyanine green) administration were also excluded. Visualization of the CNV by SSOCTA was mandatory for inclusion into the study.

Ophthalmic examination

All patients were recruited at the Department of Ophthalmology, Medical University of Vienna, Austria and followed identical standardized procedures. During the same visit, all patients underwent best-corrected ETDRS visual acuity (Told et al. 2013) testing reported as logMAR, a complete ophthalmic examination including Goldmann applanation tonometry, biomicroscopy, funduscopy, spectral domain optical coherence tomography (SDOCT) and were assessed for the diagnosis of nAMD with fluorescein and indocyanine green angiography (all Spectralis HRA + OCT, Heidelberg Engineering, Germany) previous to study inclusion. Exudative CNV activity was evaluated based on structural OCT imaging. The pupil of the study eye was dilated with eye drops containing 0.5% tropicamide.

SSOCTA evaluation

A 6 $\times$ 6 mm volumetric flow scan containing 500 $\times$ 500 A-scans was recorded with a 1060-nm swept-source OCT angiography (SSOCTA) device (PLEX Elite 9000; Carl Zeiss Meditec, Dublin, CA, USA) with an A-scan rate of 100 000 and an axial resolution of 6.3 µm. The automated layer segmentation displays the predefined vascular plexus, including the superficial and deep retinal capillary plexus as well as the outer retina to choriocapillaris (ORCC) and the choroidal capillary (CC) layer in orthogonal view. If needed, the automated layer segmentation was manually corrected using the corresponding structural B-scans to guide placement of the segmentation lines to best visualize the CNV complex. For optimal display of the CNV complex, the particular RPE – RPE fit slab or the ORCC slab (8 µm beneath Bruch's membrane to the bottom boundary of the outer plexiform layer) was used. The same visualization was used for all subsequent visits of one patient. This method allowed selection of the images that visualized the largest extent of the CNV complex in both type 1 and 2 CNV. Images had to cover the whole lesion area and were excluded if the signal-to-noise ratio was bad (<6/10) or motion artefacts or floaters were present in the area of interest.

All patients returned to the clinic for SSOCTA imaging every 7 and 14 days after aflibercept treatment as well as at days 30, 60 and 90. A subgroup of 14 patients also returned for SSOCTA imaging with dilated pupils at days 1 and 3 after treatment initiation.

Evaluation of SSOCTA-based parameters

Lesion size was determined manually by two independent graders, masked for the patient and acquisition sequence, using the Fiji 1.50e (Image J, National Institutes of Health, USA (Schindelin et al. 2012)) free-hand selection tool to calculate of the

intraclass correlation coefficient (ICC). Thereafter, the complimentary flow information surrounding the CNV lesion was masked in black to avoid this image area influencing measurements when using the AngioTool (0.6a, National Cancer Institute, USA; Zudaire et al. 2011) software. The software was used for semi-automated determination of CNV-related variables with the same setting for each patient regarding threshold, vessel thickness and removal of small particles. The tool segments, skeletonizes and analyses the explant area, which is the total area after manual delineation of the CNV complex (CNV lesion size). This area is characterized by vessel area, which is the total area with OCTA flow information within the CNV lesion, vessel density (VD) or vessel percent area, which is the percentage area of OCTA flow signal (vessels) in relation to the CNV lesion, total vessel length, which is the sum of all vessels defined as the distance between two junctions or endpoints, average vessel length, which is the average distance of all vessels defined as the distance between two junctions or endpoints, junction density, which is defined as the number of junctions per unit area, total number of junctions, the total number of vessel endpoints, defined as vessel dead ends with no continuation and lacunarity, which reflects homogeneity of vascular tissue with lower values equalling homogeneous vasculatures.

Statistical analysis

Statistical analysis was performed using Prism 6 (SoftPad Software Inc. La Jolla, CA, USA). Descriptive statistics are reported as the mean ± standard deviation (SD). ICC was calculated for delineation comparisons between graders. A repeated measurement ANOVA with Bonferoni correction was used to assess statistically significantly changes over time. The Pearson correlation was used to investigate the relationship between two variables. ETDRS VA was converted to logMAR for calculations (Khoshnood et al. 2010). Sample Size was calculated using PS Power and Sample Size Program, V3.0, 2009, Vanderbilt University, Nashville, TN, US (Dupont & Plummer 1990). Since, at the time of study planning, no data on CNV-related OCTA parameters were available, we used retinal thickness (RT) form an unpublished but similar cohort as a surrogate parameter assuming that OCTA parameters would show similar or less change. RT decreased by −3.6% compared with baseline. We consequently set δ to 1.8, σ was 3.5 resulting in a need to study 32 patients. Power was set at 0.8, and the level of significance was set to α 0.05.

Results

Patient characteristics and visual response

Thirty-two eyes of 32 consecutive patients with OCTA-positive, treatment-naïve nAMD were included in this prospective analysis. The mean patient age was 77 ± 6 years (range 58–89 years). From the 32 eyes included 16 were right eyes, 16 left eyes, 21 patients were female and 11 were male.

The mean baseline logMAR best-corrected visual acuity was 0.35 ± 0.28, ranging from 0 to 1.2 at baseline (day 0) and decreasing to 0.21 ± 0.27 ($p < 0.001$, ANOVA, see Fig. 1) after a loading dose of three monthly aflibercept injections. After the first aflibercept injection (day 30), the visual improvement was statistically significant.

Response dynamics in CNV lesion size

On average, the total CNV area increased significantly by 19.3% by day 90 after a loading dose consisting of three monthly injections. The CNV area decreased between 1 and 2 weeks after each aflibercept injection and increased thereafter in a fluctuating pattern (see Fig. 2). Compared with baseline the CNV area dropped 1 week after the first aflibercept injection by a mean of −15.4% and 2 weeks after injection by −13.6% with the largest effect of −24.8% observed 14 days after the first aflibercept injection ($p = 0.028$ paired t-test). However, after the second and third injection, this change did not reach the level of

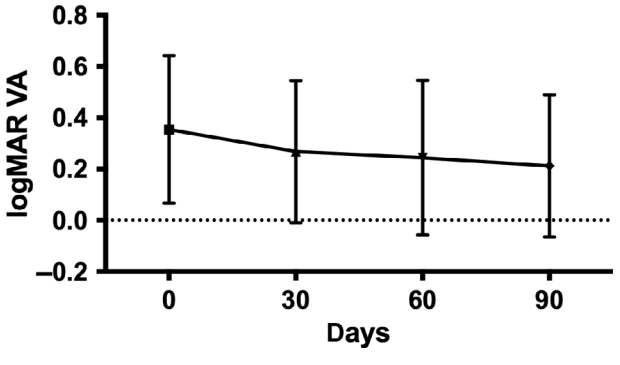

Fig. 1. logMAR visual acuity during aflibercept loading dose.

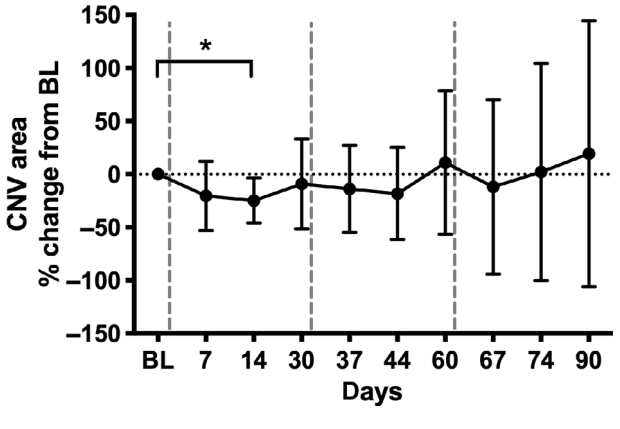

Fig. 2. Relative choroidal neovascularization area change from baseline during aflibercept loading dose. Vertical dashed lines indicate intravitreal injections; BL = baseline (day 0); The asterisk indicates a statistically significant difference based on pixel data.

significance (all $p > 0.05$). The ICC for the area measurement was 0.89.

A subgroup of 14 patients was imaged also on day 1 and 3 after the initial injection to evaluate the dynamics of early CNV reduction. As seen in Fig. 3, aflibercept had an immediate and statistically significant effect on the CNV area ($p < 0.0001$, ANOVA based on pixel data) starting at day 1 and continuing until week 2 and reaching a plateau between −21% and −28% compared with baseline.

Differentiation of subgroups in CNV response

For subgroup analysis, we graded patients according to their individual response of the CNV area to the aflibercept loading dose. This resulted in three groups: decrease of the CNV lesion by more than 50%, increase of the CNV lesion by more than 50% and an in- or decrease of the CNV lesion by <50%. Subgrouping revealed that approximately one third of the CNV lesions, either increase or decrease by more than 50% during the first three months. More than two-thirds either increased or decreased by <50% compared with BL after three months (see Table 1). These groups were pre-specified but set empirically.

Correlation of lesion area and BCVA

When the morphological and functional therapeutic response were correlated, we found that eyes with a reduction of more than 50% compared with baseline had the most prominent BCVA gain. In contrast, eyes with an increase of CNV lesion size by more than 50% showed the least functional benefit; in fact these patients showed no change in VA during the first three months. Eyes with an increase or decrease of the CNV lesion size of <50% showed a one to three line increase in VA.

We further investigated if there was a correlation between baseline lesion size and the lesion response to the aflibercept loading dose expressed by the per cent CNV area change after 3 months. Correlation analysis showed that there was a weak inverse correlation between baseline CNV area and the treatment response ($r^2 = -0.4$, $p = 0.09$). Correlation between baseline CNV area and per cent change from baseline in VA showed a non-statistically significant ($p > 0.05$) correlation of $r^2 = -0.12$.

Response of neovascular features unrelated to area

The overall vessel density of CNV lesions remained stable over time with 56.5 % at baseline and 58.4% after 3 months. There was also no significant change in VD seen following reinjections (see Fig. 5). This change was not statistically significant (all, $p > 0.05$). There was no difference in VD restructuring found between eyes, which increased or decreased by more or <50% in CNV lesion size (all $p > 0.05$).

Most of the parameters characterizing the CNV lesion showed a distinct change over time in response to aflibercept treatment. Vessel area, total vessel length, the total number of junctions and junction density responded to each aflibercept injection with a decrease after 7 to 14 days and increased thereafter until 1 month after treatment. Consistent with the change in lesion size, these effects reached the level of significance in vessel area, total vessel length and total number of junctions (all $p < 0.05$, *t*-test) following the first injection and were not statistically significant after the second and third aflibercept injection, although the dynamics showed a similar response pattern in general for several features, except VD (see Fig. 5).

However, vessel per cent area, average vessel length, total number of vessel endpoints and mean lacunarity did not show a related response pattern to aflibercept treatment, but a generally symmetric undulation not reaching statistical significant change compared with baseline (all $p > 0.05$).

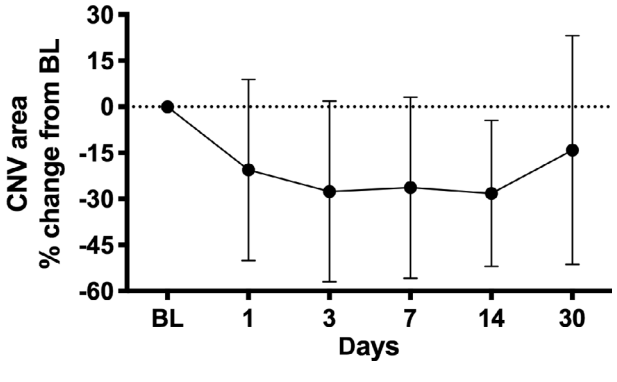

Fig. 3. The choroidal neovascularization (CNV) area as expressed by relative change form baseline. CNV reacted to aflibercept treatment with an instant decrease in size starting within 24 h continuing until day 14. BL = baseline (day 0).

Table 1. The median per cent change of choroidal neovascularization area from baseline after 3 months.

	Decrease > 50%	Decrease or increase < 50%	Increase > 50%
Median % change	−68.8%	−0.1%	107.6%
n	5 (15.6%)	23 (71.8%)	4 (12.5%)

Discussion

Pigment epithelial detachment, subretinal fluid, intraretinal fluid and central retinal thickness are OCT-based hallmarks in patients with nAMD and are used as imaging biomarkers to assess the treatment response and disease activity in clinical routine. In large-scale studies using machine learning some of these parameters, especially subretinal fluid volume in the central 3 mm and intraretinal fluid have been shown to be predictive for treatment need and visual acuity outcome (Bogunovic et al. 2017; Schmidt-Erfurth et al. 2018). With new imaging technologies such as OCTA becoming available, the search for new imaging biomarkers may reach novel horizons. SSOCTA provides high-resolution volumes of the CNV lesion, which we used to evaluate the response of vascular

morphologic biomarkers to aflibercept treatment during the particularly relevant, that is predictive time point of the loading dose. Previous studies evaluating potential OCTA biomarkers were largely cross-sectional or retrospective in nature. The focus of this prospective study was the spectrum of relevant vascular components of the CNV complex imaged with the latest generation of (SS) OCTA.

With a statistically significantly increase in visual acuity (see Fig. 1) during the loading dose, the CNV lesion area could be assumed to decrease. In fact, such a decrease in visible dimension occurs as early as at day one after anti-VEGF injection (see Fig. 3), which was equally reported by Lumbroso et al. (2015). However, over a period of three months and even following three consecutive monthly injections, the CNV area nevertheless increased statistically significantly by 19%. This is in accordance with a retrospective cohort study by Xu et al., reporting an increase of 12.5% in type 1 CNV lesions after one year of pro re nata (RPN) anti-VEGF treatment. The CNV lesion expanded even further by 25.6% compared with baseline at the last follow-up visit after a median of 16 months (Xu et al. 2018). After 12 months of anti-VEGF treatment, Sustronck et al. (2019) found an increase in CNV area of 35% in the PRN group and 25% in the treat and extend group, although the difference between groups was not statistically significant. An increase in CNV lesion size was also shown for treatment-naïve quiescent nAMD CNV lesions (Querques et al. 2013) after one year highlighting CNV growth as a natural biological behaviour (Carnevali et al. 2018). Kuehlewein et al. (2015) found no CNV area change after three months of follow-up in patients with active or chronic type 1 neovascularization, which is most likely due to the chronicity of most of the lesions included in their study. Similarly, large-scale studies such as the CATT (Martin et al. 2012), ANCHOR (Brown et al. 2006) and MARINA (Rosenfeld et al. 2006) trials showed an increase in CNV area while under continuous anti-VEGF treatment or in the sham group using fundus photography and fluorescein angiography. On the other hand, VIEW 1 and 2 showed an average decrease in CNV area after one year, but this decrease was very small with approximately 4% in all treatment groups (Heier et al. 2012). Moreover, Lumbroso et al. (2015) found a decrease in OCTA CNV lesion size 1 month after treatment initiation in only five treatment-naïve patients with type 2 nAMD. Our study offers the only larger prospective data set and includes tight timing of the early response together with the highest definition OCTA technology currently available. Our data clearly show the dynamics of neovascular change with an immediate closure of a portion of the lesion around 25% of the entire extension, most likely due to constriction than a true anatomical shrinkage of the lesion. Immediate vascular constriction has been shown as a typical reaction to VEGF blockade (Papadopoulou et al. 2009; Sacu et al. 2011). Within 2 weeks, the lesion has reopened and neovascular growth continues following the underlying VEGF stimulation. There is also clear evidence that the sensitivity to treatment diminishes already during the first injections of the loading dose.

However, not all CNV lesions are the same. Grouping the data by the level of CNV area change resulted in three groups: First, an increase and second, a decrease by more than 50% of the CNV area and third an in-or decrease by <50%. This analysis showed that approximately one third of the lesions increased or decreased by more than 50% of lesion size, and more than two-thirds of CNV lesions (71.8%) were grouped in an intermediate group, which remains in between the 50% of increase/decrease compared with baseline. Patients with a decrease in lesion size by more than 50% showed the highest gain in VA and those with an increase by more than 50% had the lowest benefit (see Fig. 4). Correlation analysis showed that there was a weak and statistically non-significant inverse correlation ($r^2 = -0.4$) between baseline CNV area and treatment response, indicating the smaller the CNV lesion at baseline the more decrease in CNV lesion size after three months of anti-VEGF treatment. Yet, there was no correlation between baseline CNV lesion size and the change of VA after 3 months, expressed as relative change from baseline.

We further evaluated quantitative intrastructural parameters characterizing the CNV vascular architecture using a semi-automated approach, which provided information on uniformity and vessel status. The current discussion of the vascular features and biology of CNV lesions per se and under anti-angiogenic therapy is extremely controversial, and the rationales are highly hypothetical: the junction number or density, for example could be a measure for angiogenic vessel sprouting; again, active lesions would be expected to show a higher junction number or density. Whereas, high values in total vessel length could either indicate CNV activity or vessel pruning due to anti-VEGF treatment resulting in the formation of vascular loops (Spaide 2015). Lacunarity, for example, might allow conclusions on the angiogenetic, that is activity status of the CNV lesion. Higher values of lacunarity might reflect an inhomogeneous CNV configuration, which is thought to be the case in old lesions with pruned vessels following arteriogenesis or after anti-VEGF injections. Similarly high values of VD were

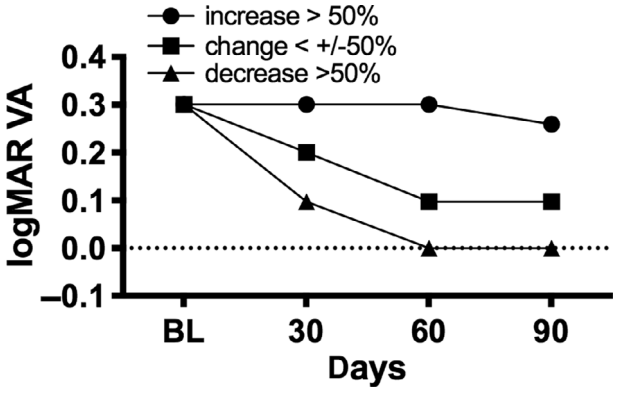

Fig. 4. Median logMAR best-corrected visual acuity change during loading dose in subgroups with in- or decreasing choroidal neovascularization area.

assumed to characterize active lesions, with abundant angiogenesis. Vessel density is defined as the relationship between vessel area and total lesion area. A retrospective and cross-sectional study previously showed that a high vessel density is considered as a feature of clinically active CNV (Coscas et al. 2018). In quiescent CNVs, VD did not increase significantly over 1 year (Carnevali et al. 2018). Our data showed that the VD of the CNV lesion did not show any characteristic, or statistically significant changes during aflibercept loading dose. The change in CNV lesion size was obviously not associated with a change in VD. In our highly standardized and homogeneous imaging analyses, we found a minimal initial decrease by 2–3% at 2 weeks after the month two and three aflibercept injection. After three months, VD had slightly but not statistically significantly increased by 4.7%. Previous findings in a PRN group showed an increase by 2% after one year. The treat and extend group decreased slightly by 4% (Sustronck et al. 2019). All these data show that VD does not decrease substantially under anti-VEGF treatment. Despite a decrease in lesion size the overall vascular activity does not seem to decrease in neovascular AMD therapy.

Further findings fit well in the context of repeated cycles of angiogenesis, the sprouting and growing of new vessels, and arteriogenesis, the dilating growth of newly formed vessels, which is due to increased flow following anti-VEGF treatment-induced regression of non-pericyte covered neovessels (Spaide 2015). Mature core vessels become protected by pericytes promoting anti-VEGF resistance (Sarks et al. 1997). Capillary regrowth resumes from these matured vessels as soon as the anti-VEGF medication wanes from the vitreous cavity. This effect can also be appreciated in Fig. 5, where vessel area, total vessel length, junctions density and total numbers of junctions decrease slightly following aflibercept injections and immediately recur with decreasing levels of anti-VEGF medications. Similarly to our study, a retrospective study showed the same response pattern when reporting the per cent change of vessel area and junctions density over 4 months in treatment-naïve patients receiving anti-VEGF loading dose (Takeuchi et al. 2018).

We could not find a specific response pattern of the CNV lesion to an aflibercept loading dose for the vessel per cent area and total number of vessel endpoints. Also, a cross-sectional study could not find a difference in lacunarity in patients responding well or badly to anti-VEGF treatment, which was defined by the interval between treatments needed to maintain a dry retina (Roberts et al. 2017). Therefore, we assume that VEGF inhibition in active CNV does inhibit leakage (Lassota et al. 2010) and induces a temporary constriction of the neovascular complex, but the vascular biology remains largely unchanged with continuous regrowth.

The limitations of our study that need to be considered are that we mainly report data expressed as relative change from baseline. This is because whether readings from OCTA images can be taken as a ground truth or a correction factor is needed, for example for absolute CNV lesion size to convert pixels into square millimetres, is still under discussion. This might induce a bias, which however would not influence the overall results of our study as we only evaluated longitudinal data and no cross-sectional comparisons were made. Furthermore, the use of automated analyses may reduce investigator-related bias in future. We tried to eliminate this effect in our study by calculating ICC for CNV area, which was delineated manually. Additionally, as we analysed a subgroup of patients with more or <50% CNV area changes, we did not group patients according to CNV type 1 or 2 or mixed type as the groups would become to small. More patients will be needed to clearly differentiate between CNV type groups in future analyses. Furthermore, we did not include CNV type 3 (Fayed & Fawzi 2019) and PCV in this study because the architecture is clearly different from type 1 and 2 nAMD CNV. This would have to be investigated in a separate study.

In conclusion, we identified and graded a morphologic response and lifecycle of the CNV lesion following aflibercept treatment during the most pronounced phase of therapy, the loading dose, using the latest generation of SSOCTA imaging and a semi-automated software approach. We confirm an immediate reaction of the CNV lesion starting within day 1 after aflibercept treatment, lasting for two weeks. Subsequently, reopening or regrowth of the lesion occurs rapidly. As early as during the second and the third treatment, resistance to anti-VEGF treatment occurs and the therapeutic response fades out. Related intralesional vascular features such as vessel area, total vessel length and total number of junctions show a similarly undulating reaction, but did not meet the same level of significance. SSOCTA baseline CNV area has no influence on VA after three months. However, the stronger the response in CNV size reduction after three months, the higher the potential increase in VA. For prognostic evaluations, it will be crucial to identify the individual condition of our patients to differentiate the subgroup of lesion

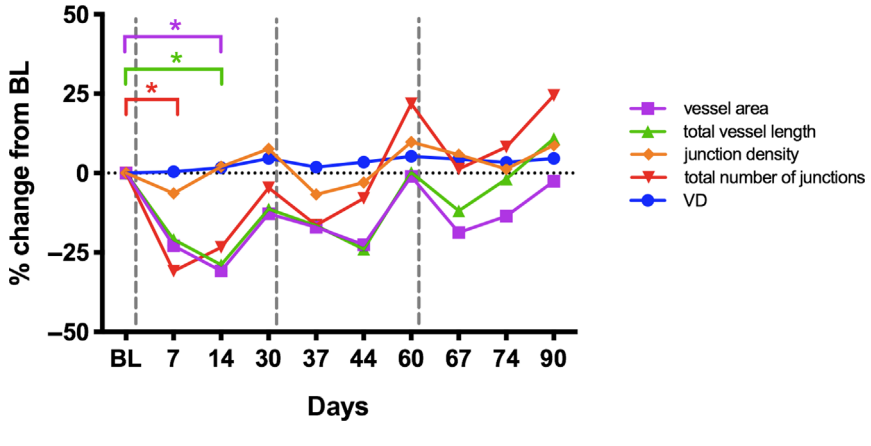

Fig. 5. Relative change from baseline shown for parameters characterizing the choroidal neovascularization area by SSOCTA: vessel density (VD), vessel area, total vessel length, total number of junctions and junctions density displayed over time (days). Vertical dashed lines indicate aflibercept treatment. Asterisks indicating significant change compared with baseline.

decrease or increase and the specific conditions, which trigger this response. However, as for clinical applicability, more has to be learned about signs of activity in SSOCTA. More than a decade after the approval of anti-VEGF for widespread clinical use, an advanced understanding of the therapeutic mechanisms may become available with SSOCTA as a valuable diagnostic companion offering the necessary insight into the vascular biology of neovascular AMD.

References

Babiuch AS, Uchida A, Figueiredo N et al. (2019): Impact of optical coherence tomography angiography review strategy on detection of choroidal neovascularization. Retina **40**: 672–678.

Bogunovic H, Waldstein SM, Schlegl T et al. (2017): Prediction of anti-VEGF treatment requirements in neovascular AMD using a machine learning approach. Invest Ophthalmol Vis Sci **58**: 3240–3248.

Brown DM, Kaiser PK, Michels M et al. (2006): Ranibizumab versus verteporfin for neovascular age-related macular degeneration. N Engl J Med **355**: 1432–1444.

de Carlo TE, Bonini Filho MA, Chin AT et al. (2015): Spectral-domain optical coherence tomography angiography of choroidal neovascularization. Ophthalmology **122**: 1228–1238.

Carnevali A, Sacconi R, Querques L et al. (2018): Natural history of treatment-naive quiescent choroidal neovascularization in age-related macular degeneration using OCT angiography. Ophthalmol Retina **2**: 922–930.

Chakravarthy U, Williams M & AMDG Group (2013): The Royal College of Ophthalmologists guidelines on AMD: executive summary. Eye (London, England) **27**: 1429–1431.

Cicinelli MV, Cavalleri M, Consorte AC, Rabiolo A, Sacconi R, Bandello F & Querques G (2019): Swept-source and spectral domain optical coherence tomography angiography versus dye angiography in the measurement of type 1 neovascularization. Retina **40**: 499–506.

Coscas F, Cabral D, Pereira T et al. (2018): Quantitative optical coherence tomography angiography biomarkers for neovascular age-related macular degeneration in remission. PLoS One **13**: e0205513.

Dupont WD & Plummer WD Jr (1990): Power and sample size calculations. A review and computer program. Control Clin Trials **11**: 116–128.

Fayed AE & Fawzi AA (2019): Projection resolved optical coherence tomography angiography to distinguish flow signal in retinal angiomatous proliferation from flow artifact. PLoS One **14**: e0217109.

Gong J, Yu S, Gong Y, Wang F & Sun X (2016): The diagnostic accuracy of optical coherence tomography angiography for neovascular age-related macular degeneration: a comparison with fundus fluorescein angiography. J Ophthalmol **2016**: 7521478.

Heier JS, Brown DM, Chong V et al. (2012): Intravitreal aflibercept (VEGF trap-eye) in wet age-related macular degeneration. Ophthalmology **119**: 2537–2548.

Jia Y, Tan O, Tokayer J et al. (2012): Split-spectrum amplitude-decorrelation angiography with optical coherence tomography. Opt Express **20**: 4710–4725.

Khoshnood B, Mesbah M, Jeanbat V, Lafuma A & Berdeaux G (2010): Transforming scales of measurement of visual acuity at the group level. Ophthalmic Physiol Opt **30**: 816–823.

Kuehlewein L, Bansal M, Lenis TL et al. (2015): Optical coherence tomography angiography of type 1 neovascularization in age-related macular degeneration. Am J Ophthalmol **160**: 739–748 e732.

Lassota N, Prause JU, Scherfig E, Kiilgaard JF & la Cour M (2010): Clinical and histological findings after intravitreal injection of bevacizumab (Avastin) in a porcine model of choroidal neovascularization. Acta Ophthalmol **88**: 300–308.

Lumbroso B, Rispoli M & Savastano MC (2015): Longitudinal optical coherence tomography-angiography study of type 2 naive choroidal neovascularization early response after treatment. Retina **35**: 2242–2251.

Martin DF, Maguire MG, Fine SL et al. (2012): Ranibizumab and bevacizumab for treatment of neovascular age-related macular degeneration: two-year results. Ophthalmology **119**: 1388–1398.

Miller AR, Roisman L, Zhang Q et al. (2017): Comparison between spectral-domain and swept-source optical coherence tomography angiographic imaging of choroidal neovascularization. Invest Ophthalmol Vis Sci **58**: 1499–1505.

Moult E, Choi W, Waheed NK et al. (2014): Ultrahigh-speed swept-source OCT angiography in exudative AMD. Ophthalmic Surgery, Lasers & Imaging Retina **45**: 496–505.

Novais EA, Adhi M, Moult EM et al. (2016): Choroidal neovascularization analyzed on ultrahigh-speed swept-source optical coherence tomography angiography compared to spectral-domain optical coherence tomography angiography. Am J Ophthalmol **164**: 80–88.

Papadopoulou DN, Mendrinos E, Mangioris G, Donati G & Pournaras CJ (2009): Intravitreal ranibizumab may induce retinal arteriolar vasoconstriction in patients with neovascular age-related macular degeneration. Ophthalmology **116**: 1755–1761.

Querques G, Srour M, Massamba N, Georges A, Ben Moussa N, Rafaeli O & Souied EH (2013): Functional characterization and multimodal imaging of treatment-naive "quiescent" choroidal neovascularization. Invest Ophthalmol Vis Sci **54**: 6886–6892.

Roberts PK, Nesper PL, Gill MK & Fawzi AA (2017): Semiautomated quantitative approach to characterize treatment response in neovascular age-related macular degeneration: a real-world study. Retina **37**: 1492–1498.

Rosenfeld PJ (2016): Optical coherence tomography and the development of antiangiogenic therapies in neovascular age-related macular degeneration. Investigative Opthalmology & Visual Science **57**: 14–26.

Rosenfeld PJ, Brown DM, Heier JS, Boyer DS, Kaiser PK, Chung CY, Kim RY & MS Group (2006): Ranibizumab for neovascular age-related macular degeneration. N Engl J Med **355**: 1419–1431.

Sacu S, Pemp B, Weigert G, Matt G, Garhofer G, Pruente C, Schmetterer L & Schmidt-Erfurth U (2011): Response of retinal vessels and retrobulbar hemodynamics to intravitreal anti-VEGF treatment in eyes with branch retinal vein occlusion. Invest Ophthalmol Vis Sci **52**: 3046–3050.

Sarks JP, Sarks SH & Killingsworth MC (1997): Morphology of early choroidal neovascularisation in age-related macular degeneration: correlation with activity. Eye **11**(Pt 4): 515–522.

Schindelin J, Arganda-Carreras I, Frise E et al. (2012): Fiji: an open-source platform for biological-image analysis. Nat Methods **9**: 676–682.

Schmidt-Erfurth U & Waldstein SM (2016): A paradigm shift in imaging biomarkers in neovascular age-related macular degeneration. Prog Retin Eye Res **50**: 1–24.

Schmidt-Erfurth U, Chong V, Loewenstein A et al. (2014): Guidelines for the management of neovascular age-related macular degeneration by the European Society of Retina Specialists (EURETINA). Br J Ophthalmol **98**: 1144–1167.

Schmidt-Erfurth U, Bogunovic H, Sadeghipour A, Schlegl T, Langs G, Gerendas BS, Osborne A & Waldstein SM (2018): Machine learning to analyze the prognostic value of current imaging biomarkers in neovascular age-related macular degeneration. Ophthalmol Retina **2**: 24–30.

Spaide RF (2015): Optical coherence tomography angiography signs of vascular abnormalization with antiangiogenic therapy for choroidal neovascularization. Am J Ophthalmol **160**: 6–16.

Sustronck P, Miere A, Nguyen D, Souied E & Oubraham H (2019): Long-term follow up of macular neovascularization using optical coherence tomography angiography: Pro Re Nata versus Treat&Extend regimens Conference poster: 124 - A0305.

Takeuchi J, Kataoka K, Ito Y, Takayama K, Yasuma T, Kaneko H & Terasaki H (2018): Optical coherence tomography angiography to quantify choroidal neovascularization in response to aflibercept. Ophthalmologica **240**: 90–98.

Told R, Baratsits M, Garhofer G & Schmetterer L (2013): Early treatment diabetic retinopathy study (ETDRS) visual acuity. Ophthalmologe **110**: 960–965.

Told R, Ginner L, Hecht A, Sacu S, Leitgeb R, Pollreisz A & Schmidt-Erfurth U (2016): Comparative study between a spectral domain and a high-speed single-beam swept source OCTA system for identifying choroidal neovascularization in AMD. Sci Rep **6**: 38132.

Told R, Sacu S, Hecht A et al. (2018): Comparison of SD-optical coherence tomography angiography and indocyanine green angiography in type 1 and 2 neovascular age-related macular degeneration. Invest Ophthalmol Vis Sci **59**: 2393–2400.

Told R, Reiter GS, Orsolya A et al. (2019): Swept source optical coherence tomography angiography, fluorescein angiography, and indocyanine green angiography comparisons revisited: using a novel deep-learning-assisted approach for image registration. Retina. https://doi.org/10.1097/IAE.0000000000002695.

Xu D, Davila JP, Rahimi M, Rebhun CB, Alibhai AY, Waheed NK & Sarraf D (2018): Long-term progression of type 1 neovascularization in age-related macular degeneration using optical coherence tomography angiography. Am J Ophthalmol **187**: 10–20.

Zotter S, Pircher M, Torzicky T, Bonesi M, Gotzinger E, Leitgeb RA & Hitzenberger CK (2011): Visualization of microvasculature by dual-beam phase-resolved Doppler optical coherence tomography. Opt Express **19**: 1217–1227.

Zudaire E, Gambardella L, Kurcz C & Vermeren S (2011): A computational tool for quantitative analysis of vascular networks. PLoS One **6**: e27385.

Received on November 13th, 2019.
Accepted on June 21st, 2020.

Correspondence:
Reinhard Told, MD, PhD
Department of Ophthalmology and Optometry
Medical University of Vienna
Währinger Gürtel 18-20
1090 Vienna
Austria
Tel: +43 (0)1 40400-79310
Fax: +43 (0)1 40400-79320
Email: reinhard.told@meduniwien.ac.at

Schmidt-Erfurth: Consultancy for Bayer, Boehringer, Genentech, Kodiak, Novartis, Roche